

NASA
Reference
Publication
1104

9
Y

May 1983

Perfect Bell Nozzle Parametric and Optimization Curves

J. L. Tuttle
and D. H. Blount



(NASA-EP-1104) PERFECT BELL NOZZLE
PARAMETRIC AND OPTIMIZATION CURVES (NASA)
32 p HC AC3/MF A01

N83-24549

CSCI 21H

H1/20 Unclassified
03625

NASA



**NASA
Reference
Publication
1104**

1983

Perfect Bell Nozzle Parametric and Optimization Curves

**J. L. Tuttle
and D. H. Blount**

*George C. Marshall Space Flight Center
Marshall Space Flight Center, Alabama*

9
Y

TABLE OF CONTENTS

	Page
INTRODUCTION.....	1
NOZZLE DESIGN	1
NOZZLE DATA	2
NOZZLE OPTIMIZATION.....	2
CONCLUSIONS	3
REFERENCES	26

PRECEDING PAGE BLANK NOT FILMED

LIST OF ILLUSTRATIONS

Figure	Title	Page
A.	Illustration of optimum nozzles for given constraints	6
1.	Perfect nozzle shapes	7
2.	L/D_t versus A_D ($10 < A_D < 180$)	8
3.	L/D_t versus A_D ($100 < A_D < 2000$)	9
4.	L/D_t versus A_D ($1000 < A_D < 6100$)	10
5.	A_s/A_t versus A_D ($10 < A_D < 150$)	11
6.	A_s/A_t versus A_D ($100 < A_D < 3000$)	12
7.	A_s/A_t versus A_D ($1000 < A_D < 6100$)	13
8.	THETA versus A_c/A_t	14
9.	A_e/A_t versus P_e/P_c ($10 < A_D < 80$)	15
10.	A_e/A_t versus P_e/P_c ($80 < A_D < 6100$)	16
11.	ETA_n versus A_D ($10 < A_D < 180$)	17
12.	ETA_n versus A_D ($100 < A_D < 1480$)	18
13.	ETA_n versus A_D ($1000 < A_D < 6100$)	19
14.	A_D versus A_e/A_t for maximum ETA_n	20
15.	L/D_t versus A_e/A_t for maximum ETA_n	21
16.	A_D versus A_e/A_t for minimum A_s/A_t nozzles	22
17.	L/D_t versus A_e/A_t for minimum A_s/A_t nozzles	23
18.	A_D versus A_e/A_t for minimum L/D_t nozzles	24
19.	L/D_t versus A_e/A_t for minimum L/D_t nozzles	25

DEFINITION OF SYMBOLS

A_D	Ratio of design exit area to throat area
$A_e/A_t,\epsilon$	Ratio of exit area to throat area
A_s/A_t	Ratio of contour surface area to throat area
Y/R_t	Ratio of radial distance from centerline to throat radius
L/R_t	Ratio of axial distance from throat to throat radius
L/D_t	Ratio of axial distance from throat to throat diameter
P_e/P_c	Ratio of exit pressure to chamber (total) pressure
ETA_n	Nozzle efficiency
γ	Gas specific heat ratio, gamma
C_{fg}	Two-dimensional thrust coefficient without friction
C_{fn}	Two-dimensional thrust coefficient with friction
C_{fi}	One-dimensional isentropic thrust coefficient
THETA	Angle between contour and centerline (deg)

REFERENCE PUBLICATION

9
Y

PERFECT BELL NOZZLE PARAMETRIC AND OPTIMIZATION CURVES

INTRODUCTION

Parametric nozzle performance data for bell nozzles are often required in the analysis and trade studies of rocket engines. In order to get accurate comparisons, it is very important to have a consistent set of data which covers the entire range of area ratios and nozzle lengths allowable. Although these data are available (in fragmented form) over a fairly wide range of area ratios, new high performance/high pressure space engine applications require these data at area ratios well above those considered in the past. This document presents design data for untruncated nozzle expansion area ratios from 10 to 6100 for a specific heat ratio, (γ) of 1.2 and includes curves which permit the optimization of nozzles for maximum thrust coefficient within a given length, surface area or area ratio.

NOZZLE DESIGN

The computer code documented in Reference 1 was used to perform the calculations for this report. The nozzle contours are constructed using the "method of characteristics" which is detailed in many texts such as Reference 2 and are of the wind tunnel or "perfect" nozzle type. These perfect bell nozzles are two-dimensional axisymmetric (i.e., all properties can be specified by two dimensions: axial distance downstream from the throat and radial distance from the centerline). They have the imposed constraint that the flow field velocity vectors at the nozzle exit (untruncated design area ratio, A_D) be of uniform magnitude and parallel to the centerline. Three thrust coefficients are calculated by the code for vacuum external conditions. They are the gross thrust coefficient, C_{fg} , which is found by integrating the momentum and pressure force across the throat and then adding the thrust due to pressure on the nozzle wall; the net thrust coefficient, C_{fn} , which is found by calculating the wall shear force (drag) caused by friction and subtracting it from the gross thrust; and the ideal thrust coefficient, C_{fi} , which is found by evaluating the one-dimensional isentropic flow equations at the given area ratio. A nozzle efficiency factor ETA_n , is defined as C_{fn}/C_{fi} and is used to convert ideal thrust coefficients (and thereby one-dimensional isentropic specific impulse) to the actual two-dimensional axisymmetric case with friction. Since the wall friction is only applied to find the net thrust coefficient after the frictionless nozzle contour has been determined, it does not affect the contour or surface area.

A description of the input required by the nozzle design code is shown in Table 1. The actual input values used to generate the data for the curves are shown in Table 2. Slight changes in the number of points on the centerline and exit radius were necessary to successfully execute the code for different ranges of the design area ratio, A_D . A corner expansion was chosen since it yields shorter nozzles than ones with a radius downstream of the throat for any given area ratio. Although the friction factor would depend on wall smoothness and the Reynolds number which is a function of combustion product density, nozzle size, and the viscosity of the combustion products, a value of 0.003 Fanning (0.012 Darcy-Weisbach) was chosen as representative. Large, high pressure nozzles would have a little lower and small, low pressure nozzles a little higher friction factor.

NOZZLE DATA

The nozzle contours produced by the design procedures above are shown in Figure 1 where the radial distance from the centerline, Y , and the distance downstream from the throat, L , are normalized by the throat radius, R_t . The untruncated design area ratio, A_D , represents the area ratio where uniform, parallel flow has been achieved for that contour. Since these nozzles are very long and derive very little thrust from the nearly parallel walls near their exit, the nozzles are nearly always truncated to a smaller area ratio as discussed later. The contours for A_D 's of 600 and larger are of course not shown to completion in this figure and the somewhat erratic values are the results of convergence tolerance as the code iterated to obtain the desired input values. It should be noted that only the A_D need be specified to define a nozzle contour and only two of the three variables Y/R_t (which is $\sqrt{\epsilon}$), L/R_t and A_D need to be specified to fully define a truncated nozzle. To enable a comparison of the performance of the different contours, lines of constant net thrust coefficient, C_{fn} , (which includes friction) and wall surface area normalized to throat area, A_s/A_t , are superimposed. Although Figure 1 gives a good visualization of the nozzle contours and performance comparison it is sometimes difficult to accurately read data from it.

Figures 2 through 8 give improved resolution and interpreting capability. Figures 9 and 10 present the internal wall pressure normalized by chamber pressure (i.e., total pressure since the calculations are for isentropic flow). This is the pressure that is integrated along the wall to find the wall thrust contribution. The important nozzle efficiency, C_{fn}/C_{fi} , which was discussed above in the nozzle design section is presented in Figures 11 through 13. Note that the efficiency has a maximum value for each area ratio. Since the one-dimensional, frictionless, ideal thrust coefficient is constant for a given area ratio, there is an A_D contour which produces a maximum thrust for a given area ratio. In other words, a set of nozzles exists which produce a maximum thrust for a given area ratio. This is covered further in the next section.

NOZZLE OPTIMIZATION

An Optimization Process is used to determine where to truncate the full nozzle contour to obtain maximum thrust (i.e., $\max C_{fn}$) within a given constraint such as nozzle area ratio (or diameter), surface area, or length. This optimization is best visualized by considering an enlarged section of Figure 1 shown in Figure A. Point "a" on the figure, which is the point where the net thrust coefficient, C_{fn} , line is tangent to a line of constant Y/R_t (or area ratio, ϵ), is the optimization representing the exit point of a nozzle contour yielding maximum thrust for a given area ratio or diameter. This is the optimization mentioned in the preceding section and as discussed there is also the point of maximum nozzle efficiency as seen in Figures 11 through 13. These points have been replotted on Figures 14 and 15 to enable nozzles of this set to be easily defined. Similarly, point b, the point at which the C_{fn} line is tangent to the constant surface area line, A_s/A_t , represents the optimization of maximum thrust for a given surface area. This set is given in Figures 16 and 17. Nozzles of maximum thrust for a given length are represented by point C and curves for this set are shown in Figures 18 and 19. These minimum length optimized nozzle will be of a slightly different contour than the Rao minimum length nozzles [3] because the Rao nozzles do not have the added constraint which requires uniform parallel flow at the

9
Y

untruncated design area ratio. The actual difference in performance at a given length will be very small between the two design methods, and the family of perfect bell nozzles has the advantage of including data for the other optimized sets of minimum surface area and maximum efficiency for a given area ratio as well as any other nozzles up to the untruncated wind tunnel nozzle. Point "d" on Figure A represents the most thrust obtainable from any given nozzle contour, A_D . When the nozzle contour extends beyond this point, wall friction forces become greater than the pressure forces netting a negative thrust contribution which decreases the total thrust. This set of nozzles is not of practical interest, however, because the set of nozzles represented by point "a" are both shorter and have smaller diameters for the same thrust.

CONCLUSIONS

Use of the optimization curves allows selection of nozzle contours with certain desired characteristics and comparison of nozzles of one optimum set to others. Minimum length perfect Bell nozzles are similar in contour and performance to the minimum length nozzles designed by the Rao optimization method.

**ORIGINAL PAGE IS
OF POOR QUALITY**

**TABLE 1. BELL NOZZLE DESIGN PROGRAM INPUT DESCRIPTION
PERFECT GAS MODEL OPTION
GAMMA = 1.2**

Variable	Default Value	Description
FCON	1.0	FCON = 1.0 for two-dimensional axisymmetric flow FCON = 0.0 for two-dimensional plane flow
R	0.0	Normalized radius of circle (R/R_t) for circular expansion $R = 0.0$ for corner expansion
XNSL	0.0	Number of streamlines to be calculated
CYLHT	0.01	Ratio of cylinder radius to throat radius
XN1	20.0	Number of points on starting line
XNE	60.0	Number of points on exit Mach line
DLX	0.1	Maximum distance between adjacent Mach lines along the cylinder normalized by throat radius ($\Delta X/T_t$)
ATOL	0.0005	Iteration tolerance on design area ratio
PITOL2	0.005	Maximum increment of $\tan \theta$ for corner or circular expansion
FM	1.005	Starting line Mach number for uniform flow
CF1	0.003	Incompressible coefficient of skin friction along nozzle contour
DRAG 1	0.011	Thrust loss at the throat
TOLI	0.00001	Iteration tolerance for interior point
PA	0.0	Ambient pressure ratio (Pa/Pc)

TABLE 2. PERFECT BELL NOZZLE PARAMETRIC AND OPTIMIZATION ANALYSIS INPUT VALUES

Design Area Ratio Range	Variables											
	F C O N	X N S L	C Y H T	X N I	X N E	D L X	A T O L	P I T O L 2	C F 1	D R A G 1	T O L 1	P A
10 - 180	1.0	0.0	0.0	0.01	70.	150.	0.1	7.5×10^{-4}	7.5×10^{-3}	1.005	0.003	0.011×10^{-5}
220 - 600					150.	300.	0.3					
700					300.	800.	0.5					
800 - 900					70.	150.	5.					
1000					70.	500.	30.					
1500 - 60000					70.	500.	30.	0.0301				

ORIGINAL PAGE IS
OF POOR QUALITY

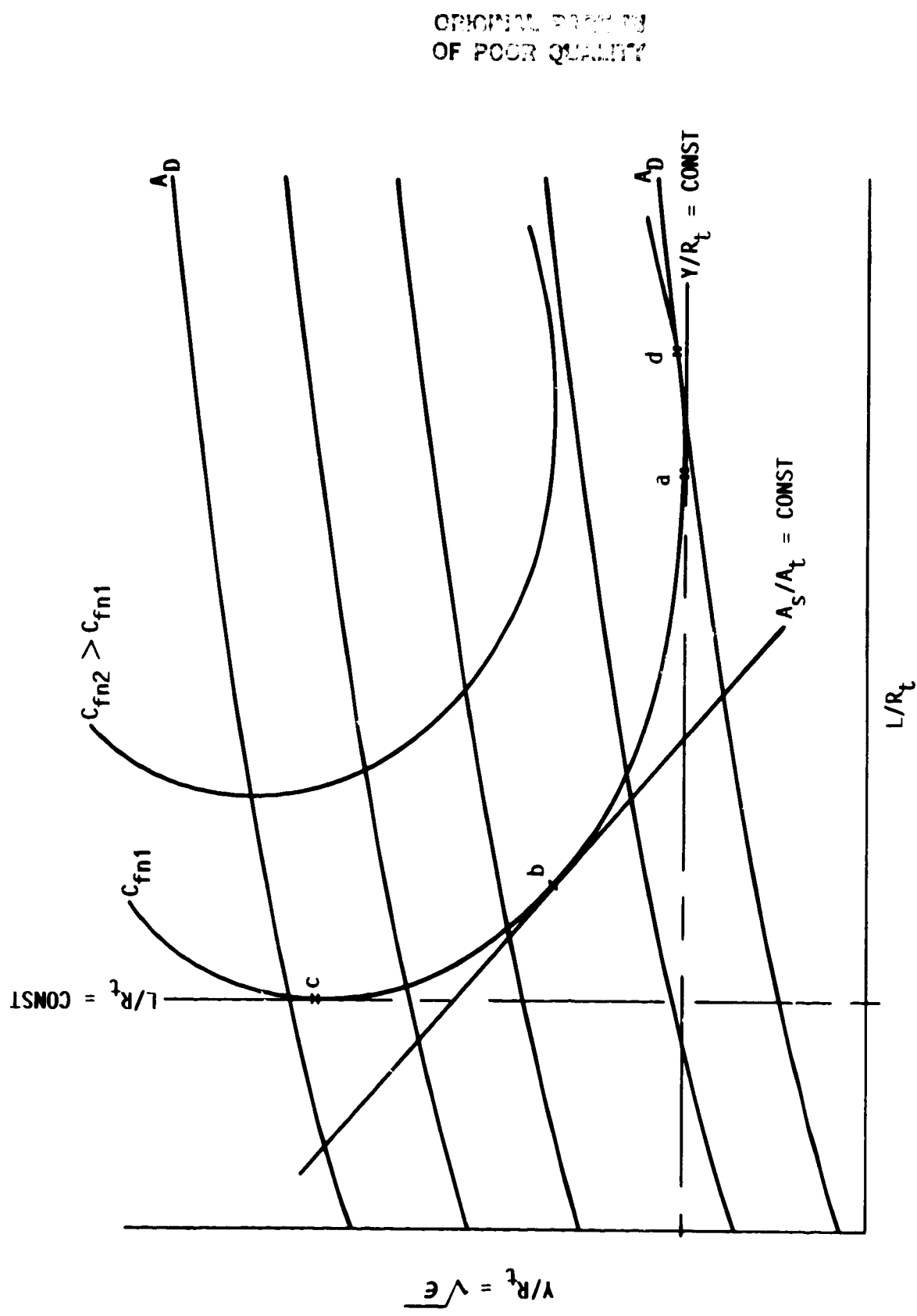
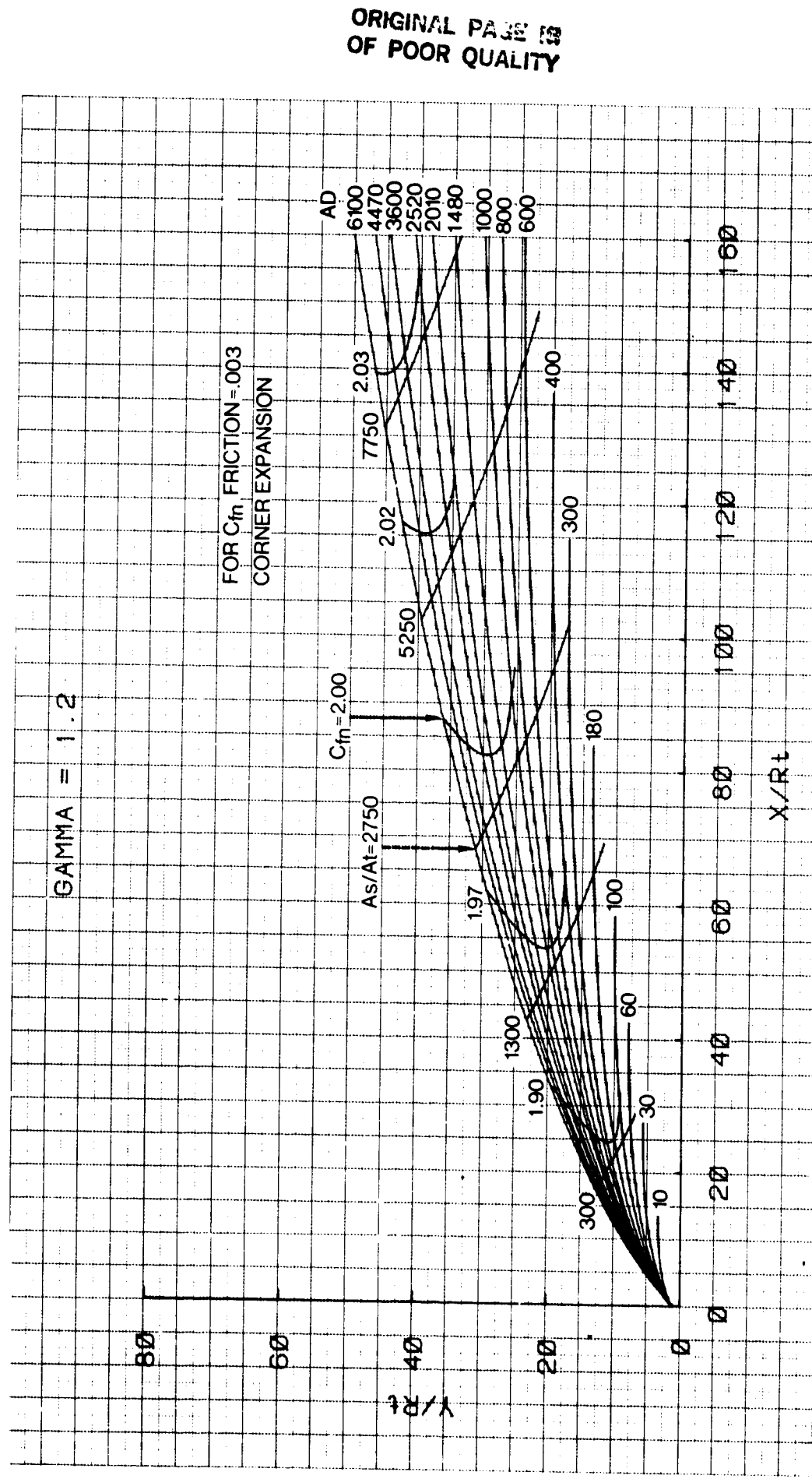


Figure A. Illustration of optimum nozzles for given constraints.



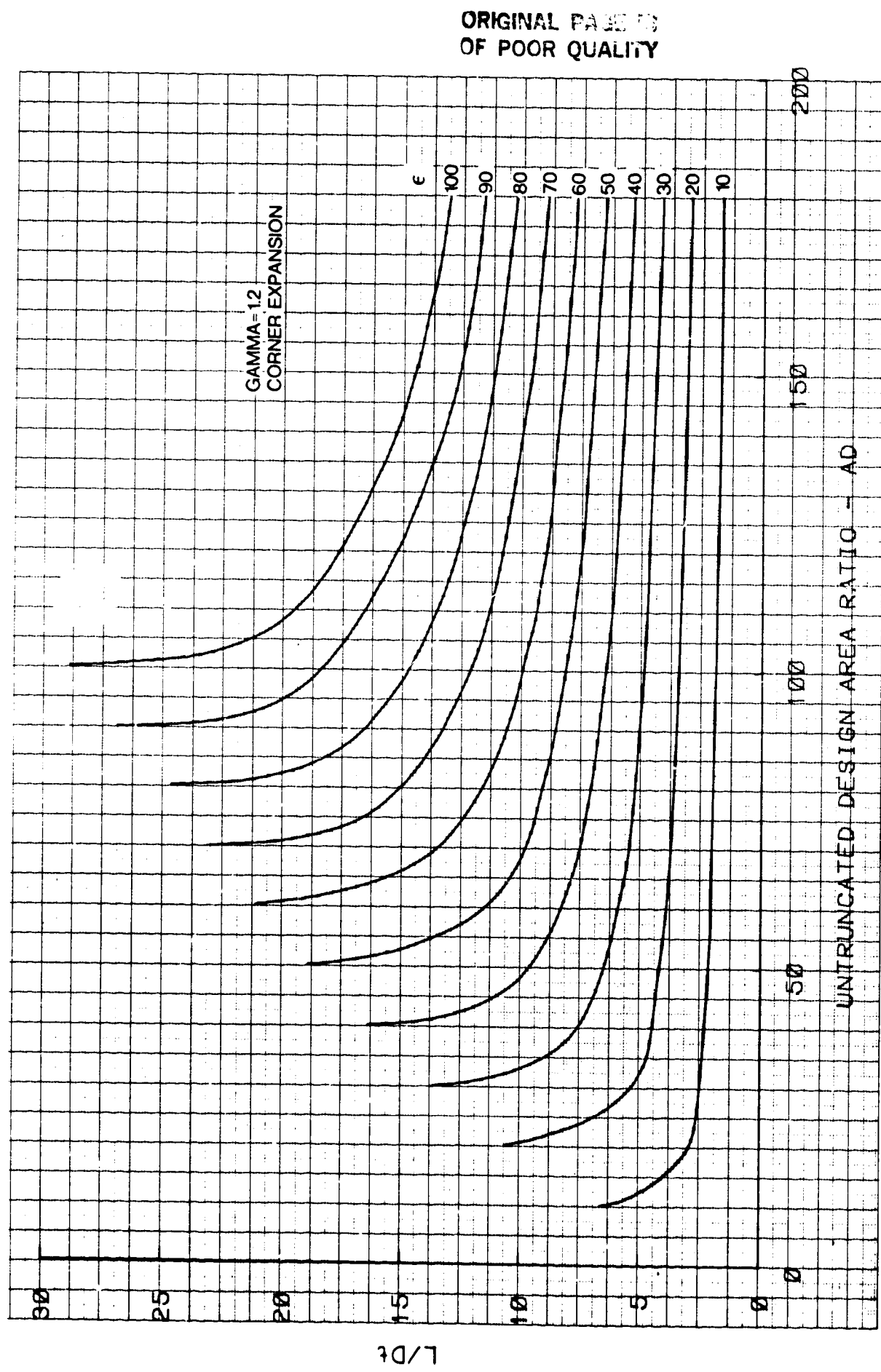


Figure 2. L/D_t versus A_D

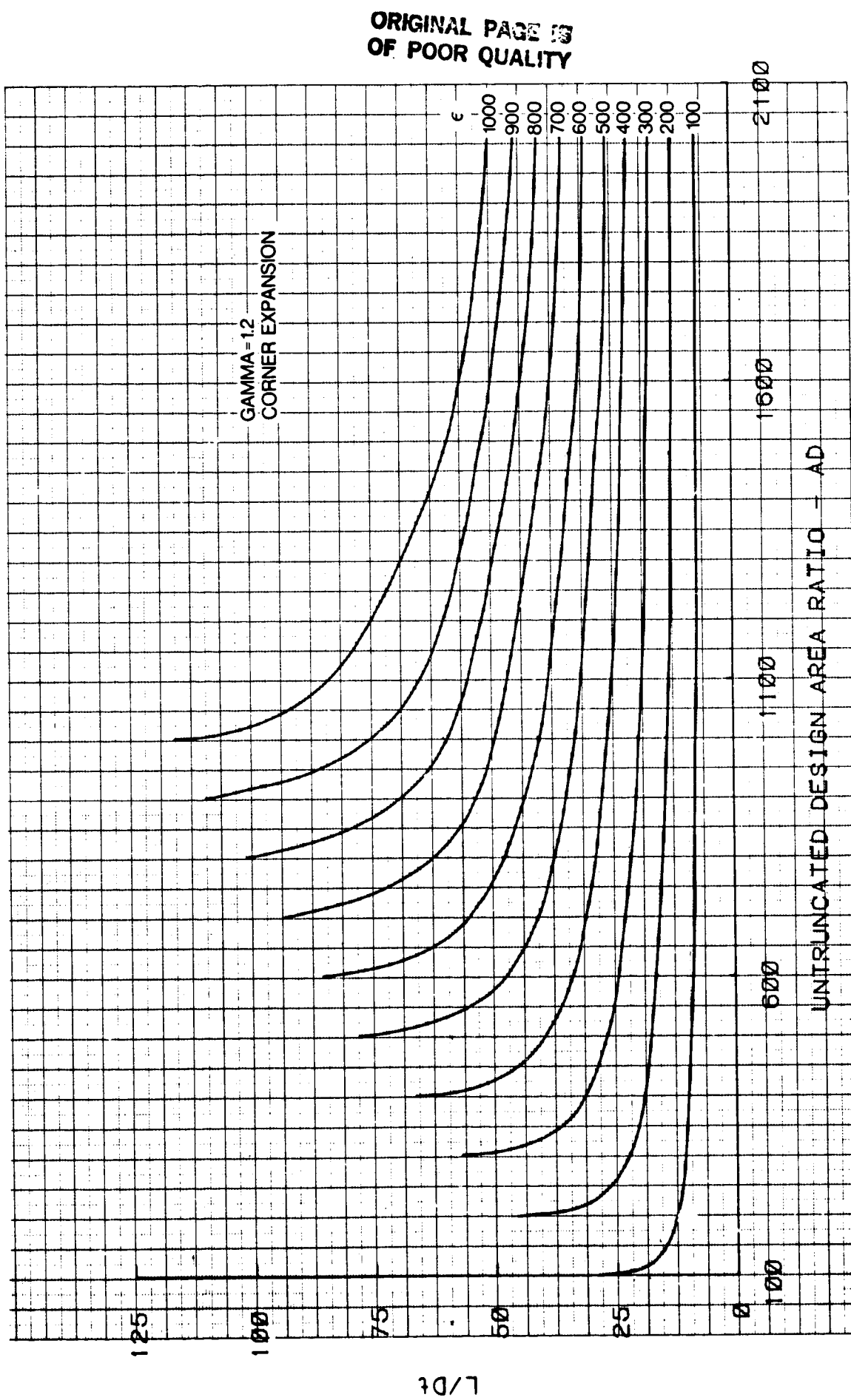


Figure 3. L/D_t versus A_D

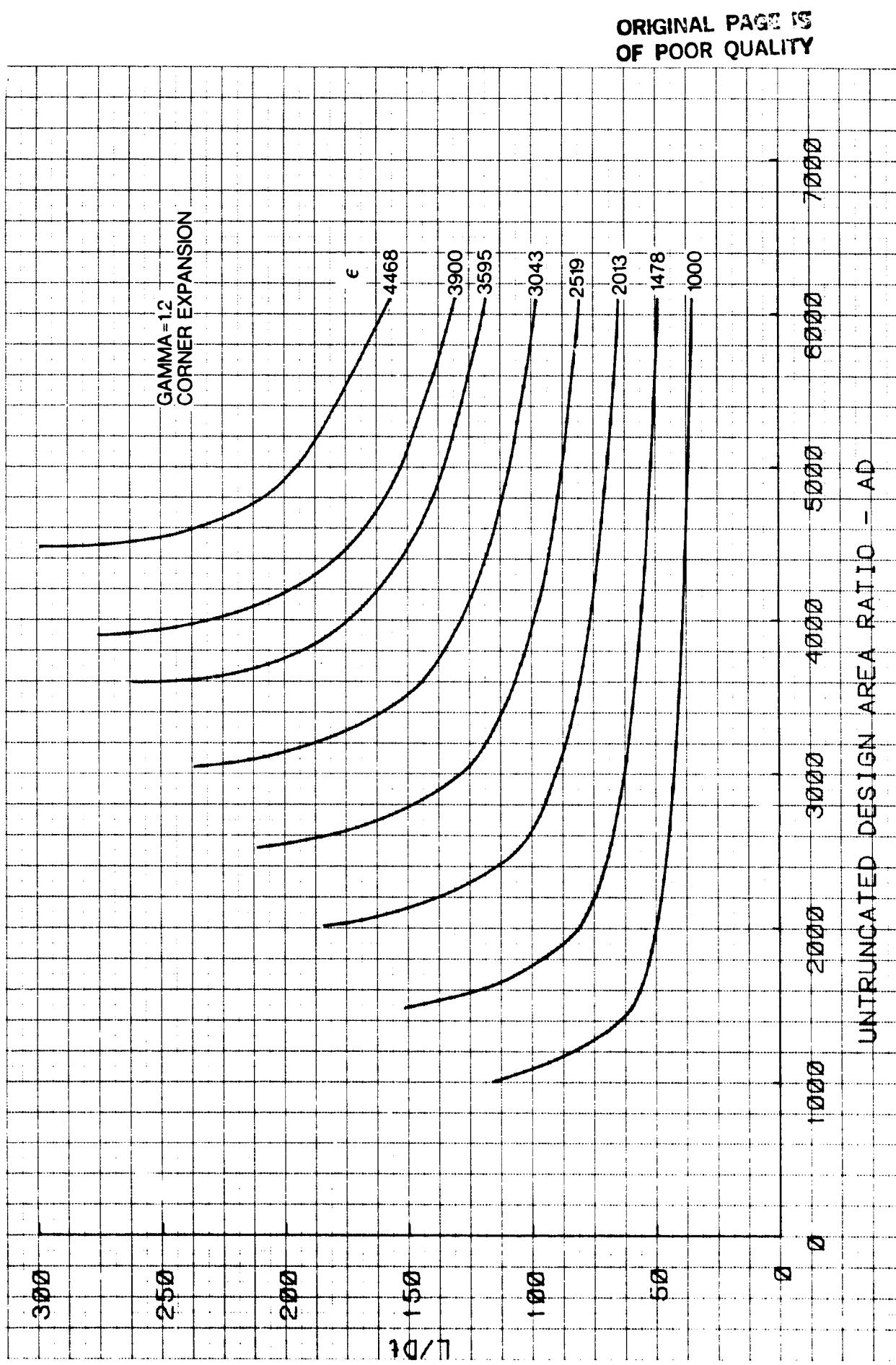


Figure 4. L/D_t versus AD

ORIGINAL PAGE IS
OF POOR QUALITY.

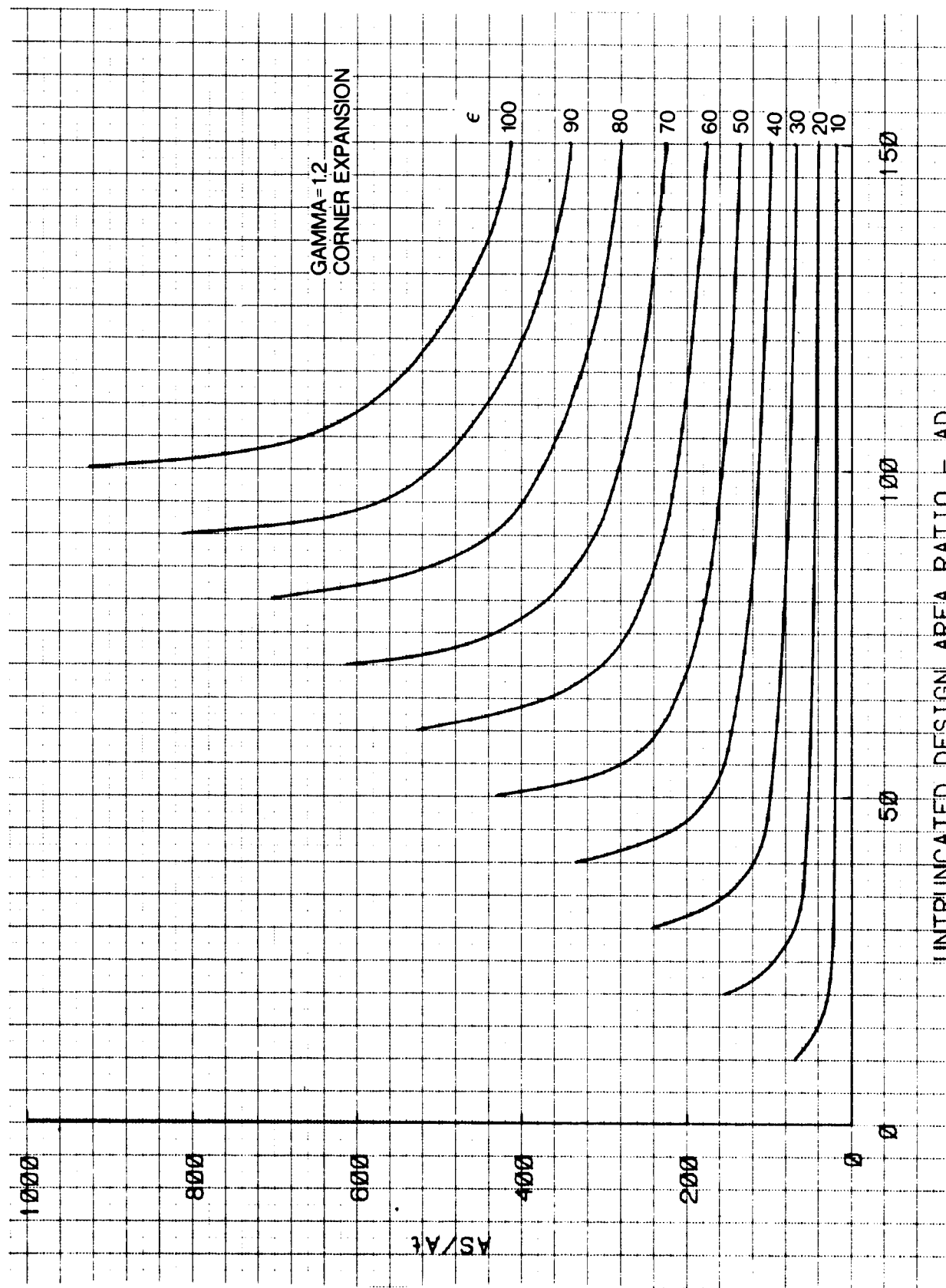


Figure 5. A_s/A_t versus A_D

ORIGINAL PAGE IS
OF POOR QUALITY

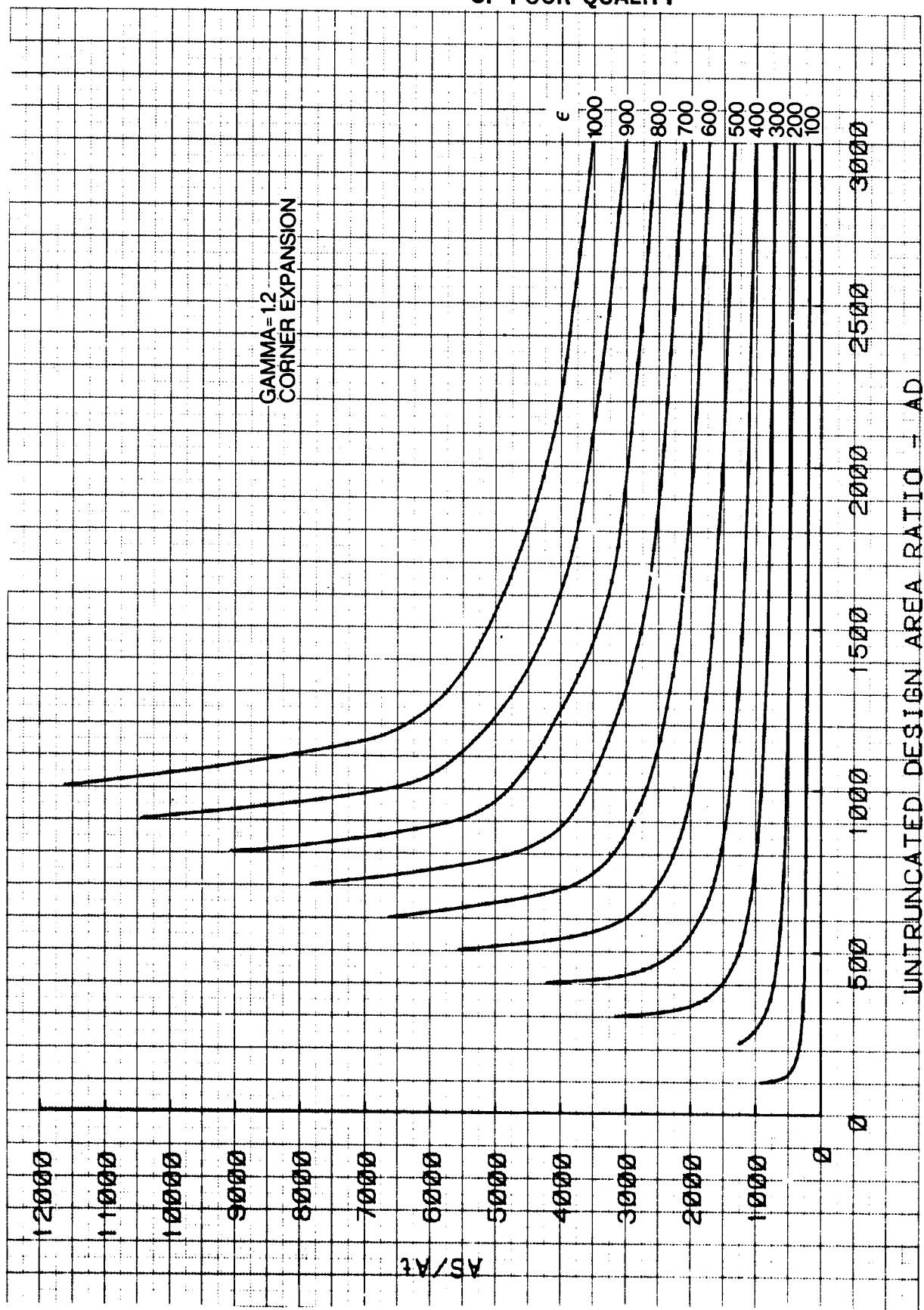


Figure 6. A_s/A_t versus AD

ORIGINAL PAGE IS
OF POOR QUALITY

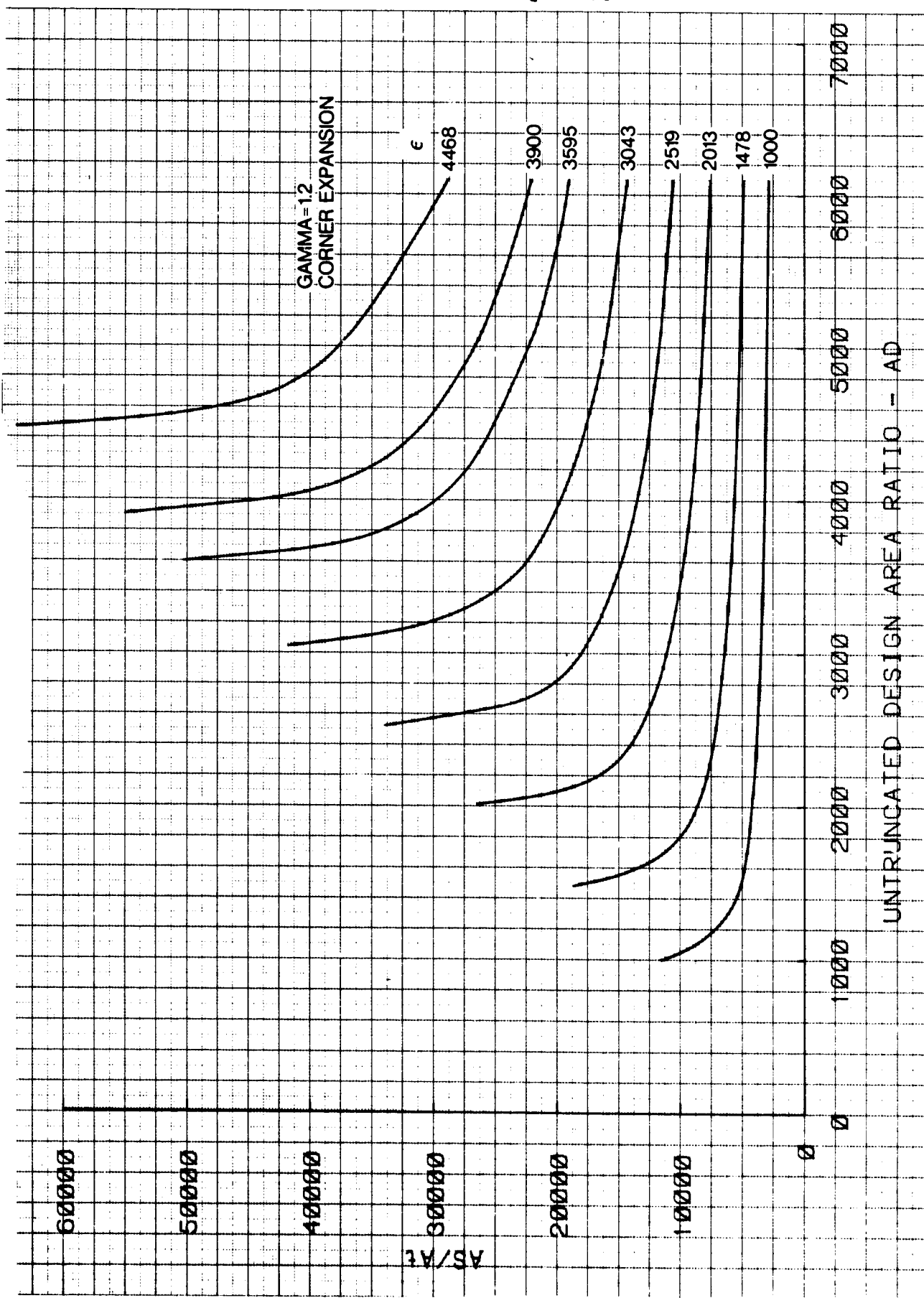


Figure 7. A_s/A_t versus AD

ORIGINAL PAGE IS
OF POOR QUALITY

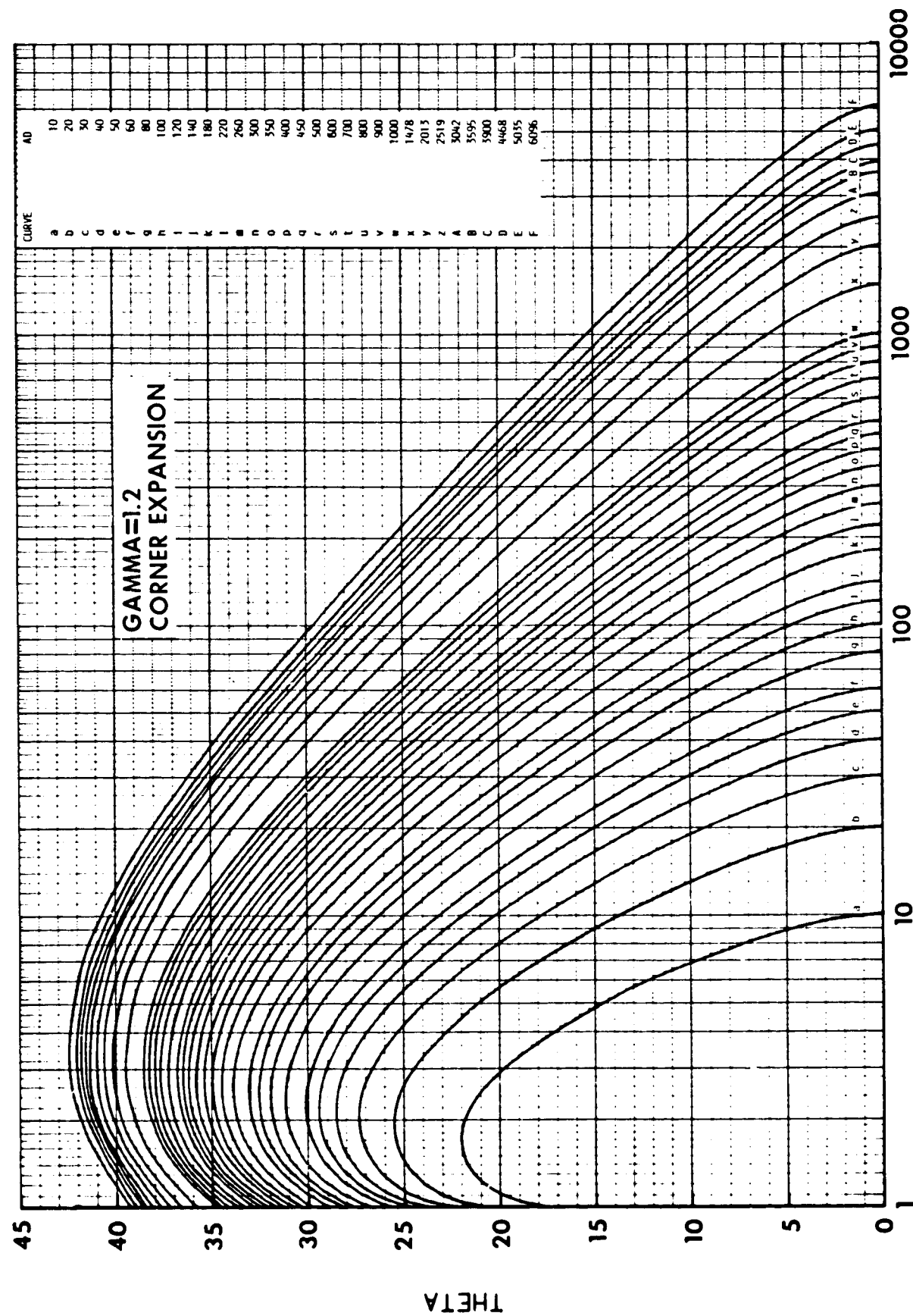


Figure 8. THETA versus A_e/A_t

ORIGINAL PAGE IS
OF POOR QUALITY

49

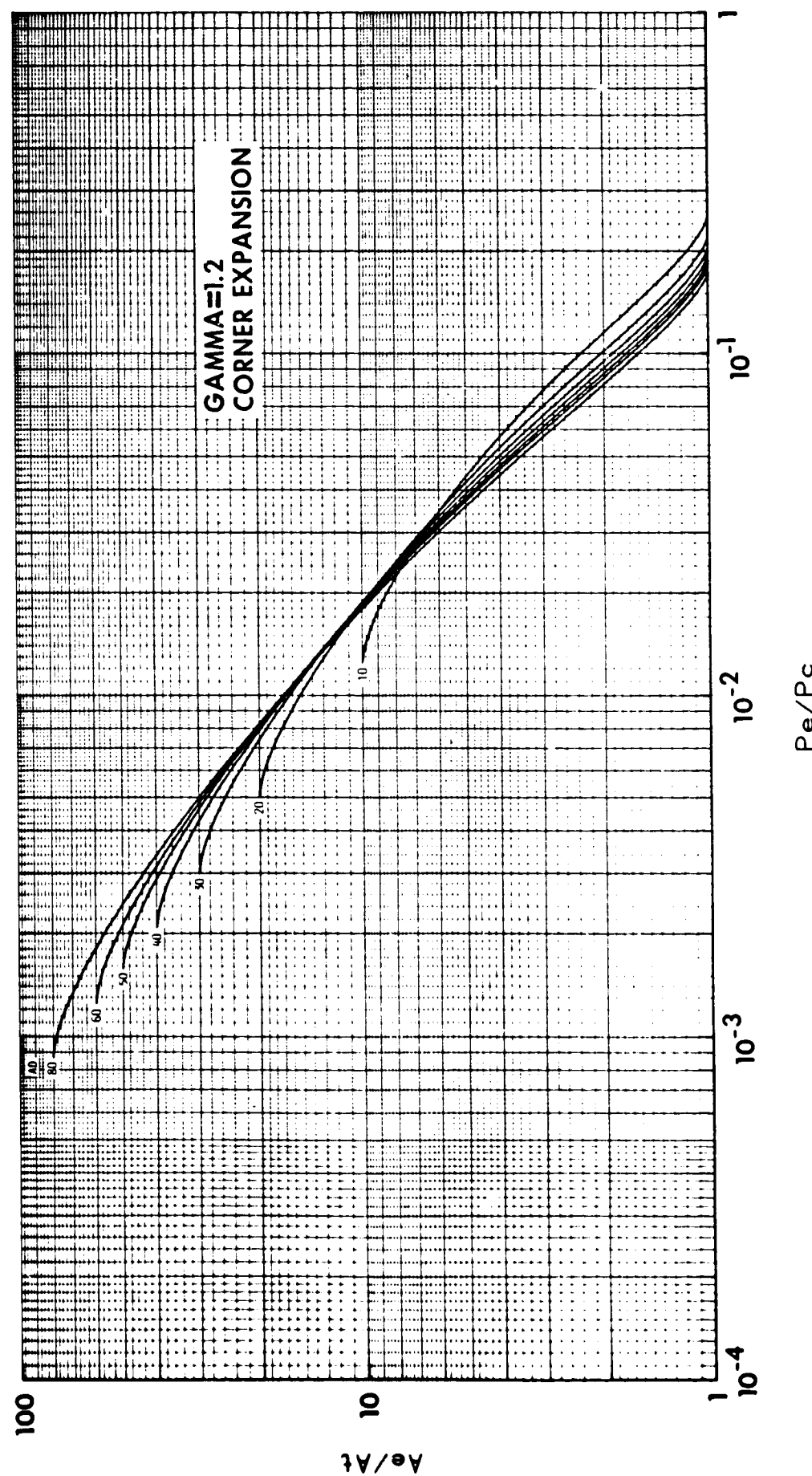


Figure 9. A_e/A_t versus P_e/P_c

ORIGINAL PAGE IS
OF POOR QUALITY

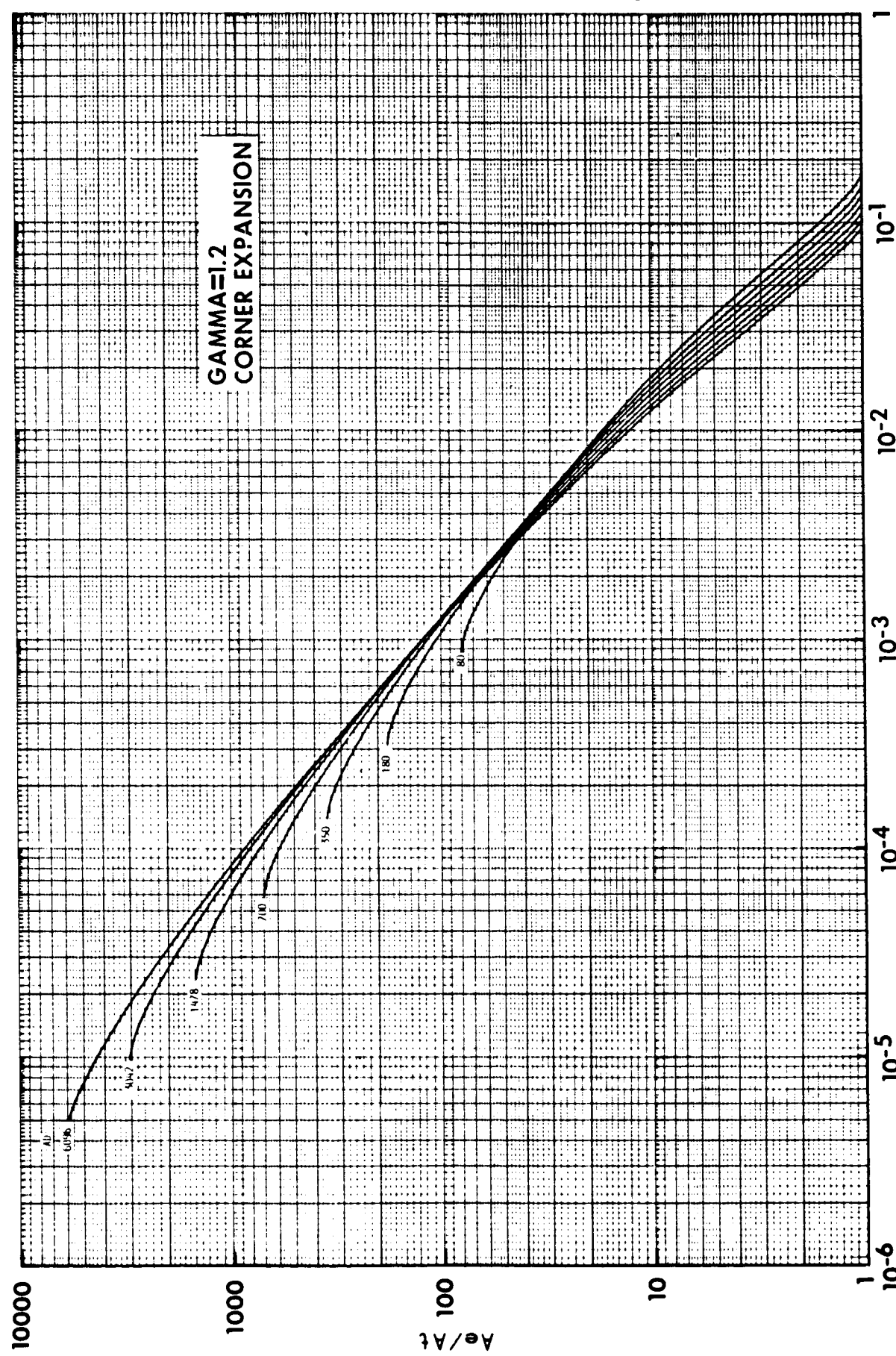


Figure 10. A_e/A_t versus P_e/P_c

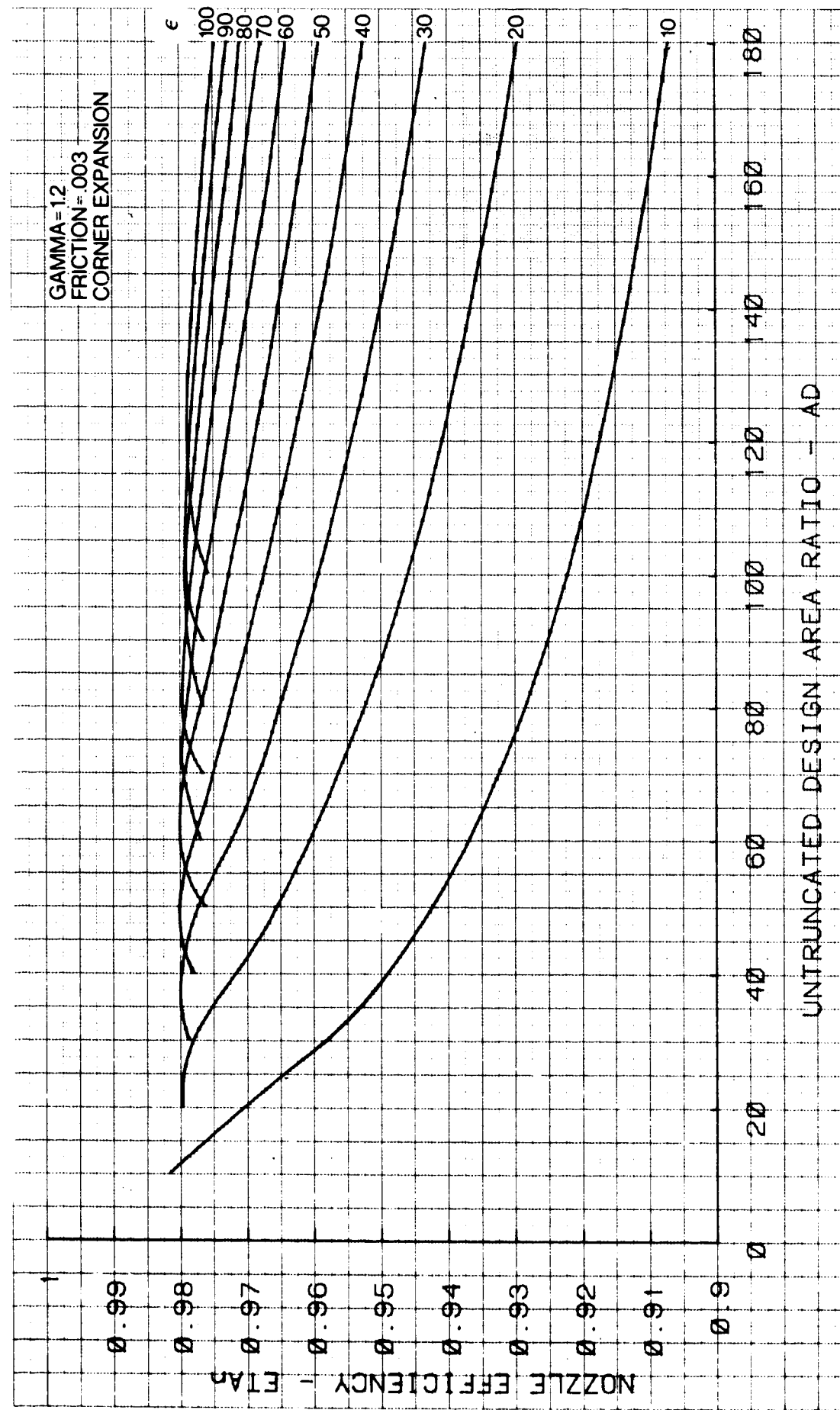


Figure 11. η_{TA} versus AD

ORIGINAL PAGE IS
OF POOR QUALITY

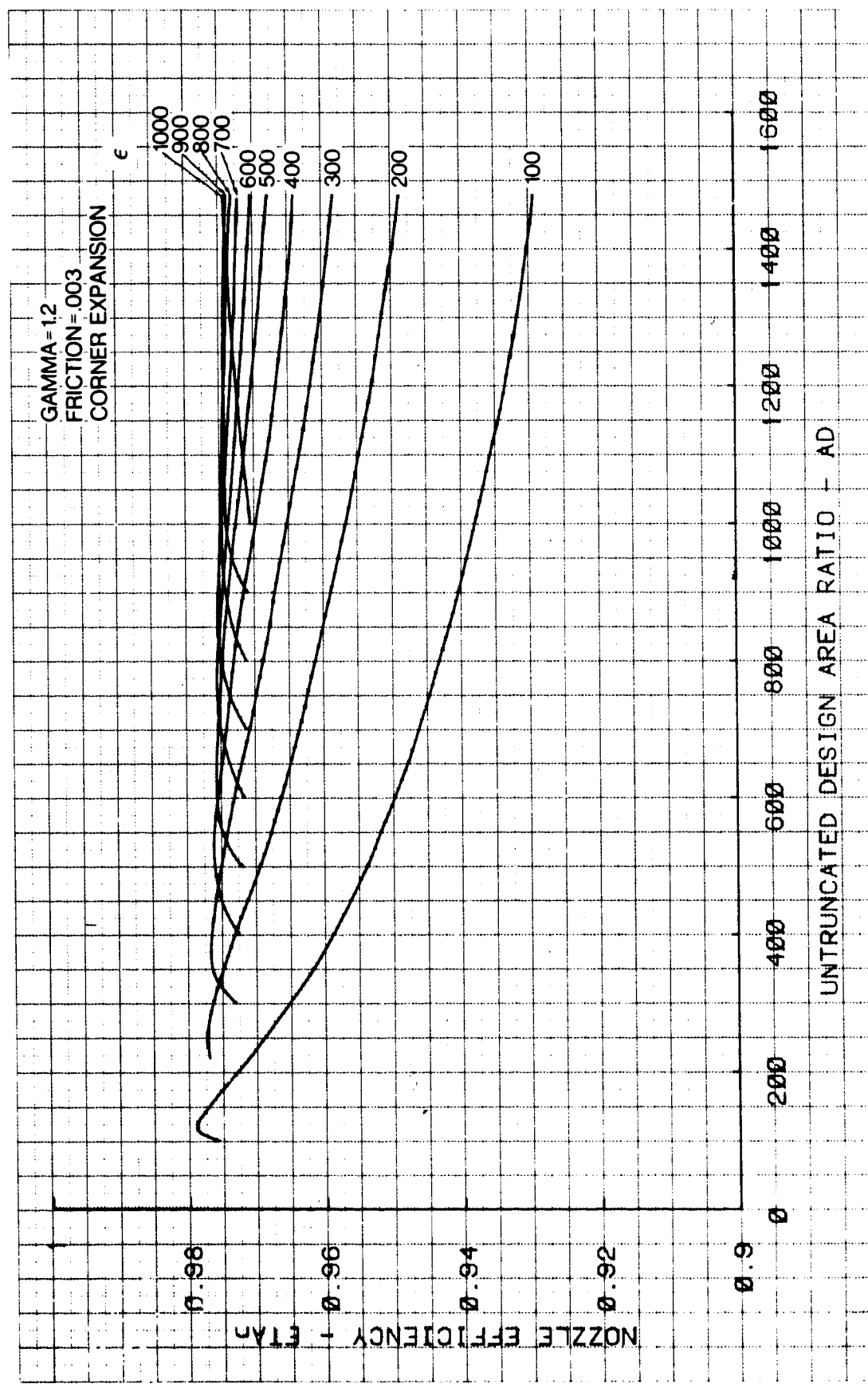


Figure 12. ETA_n versus A_D

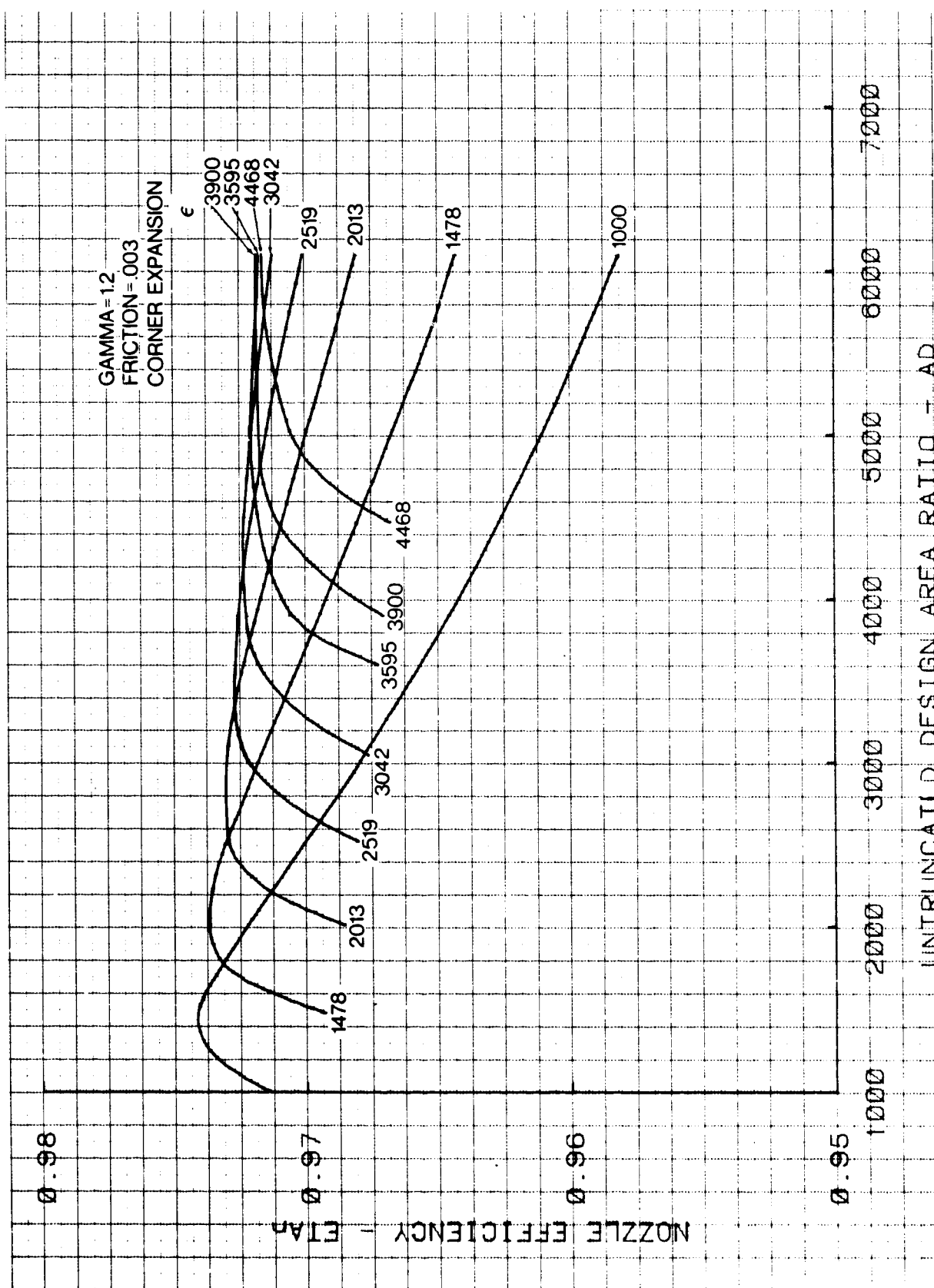


Figure 13. ETA_{η} versus AD

ORIGINAL PAGE IS
OF POOR QUALITY

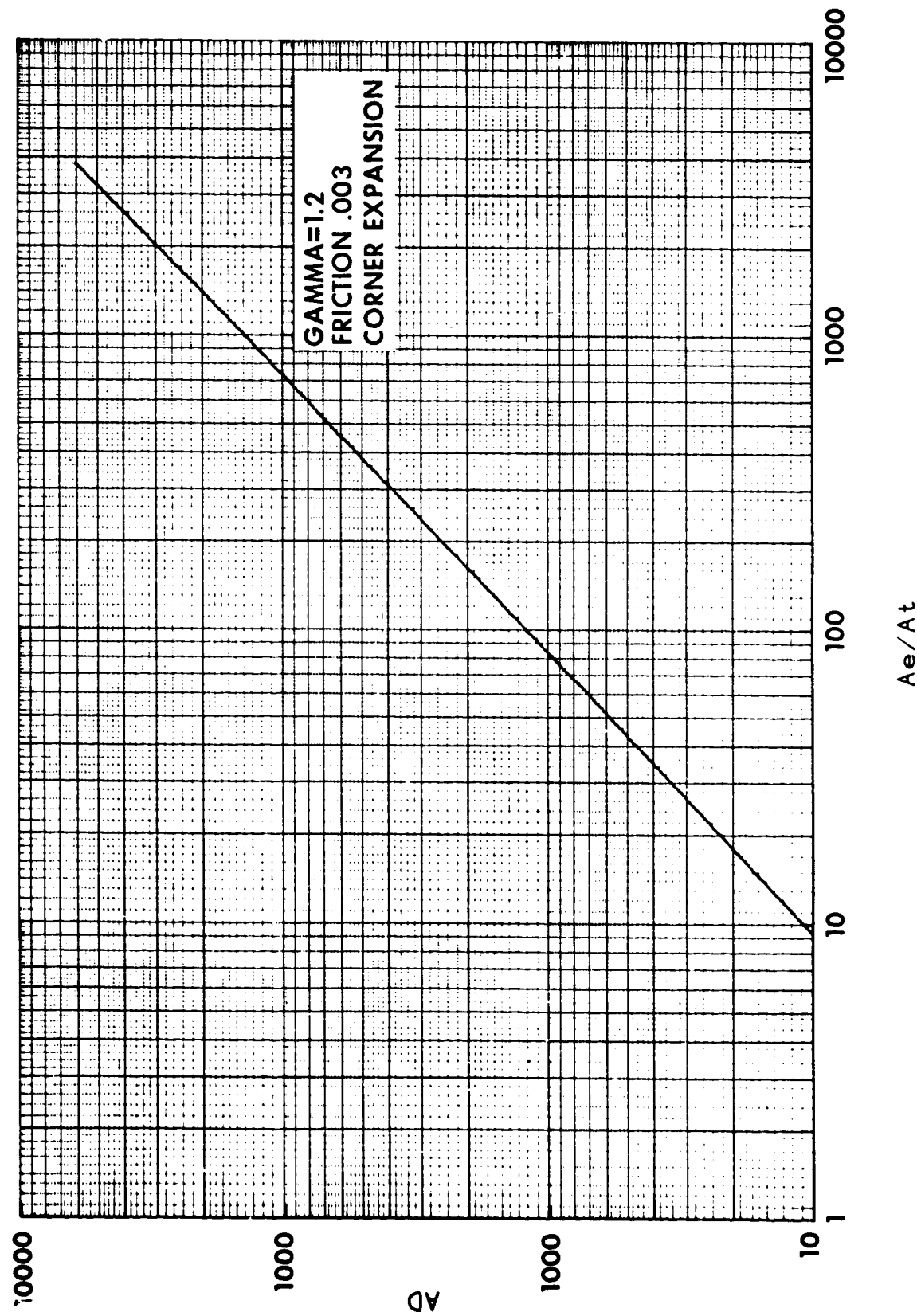


Figure 14. A_D versus A_e / A_t for maximum η_A .

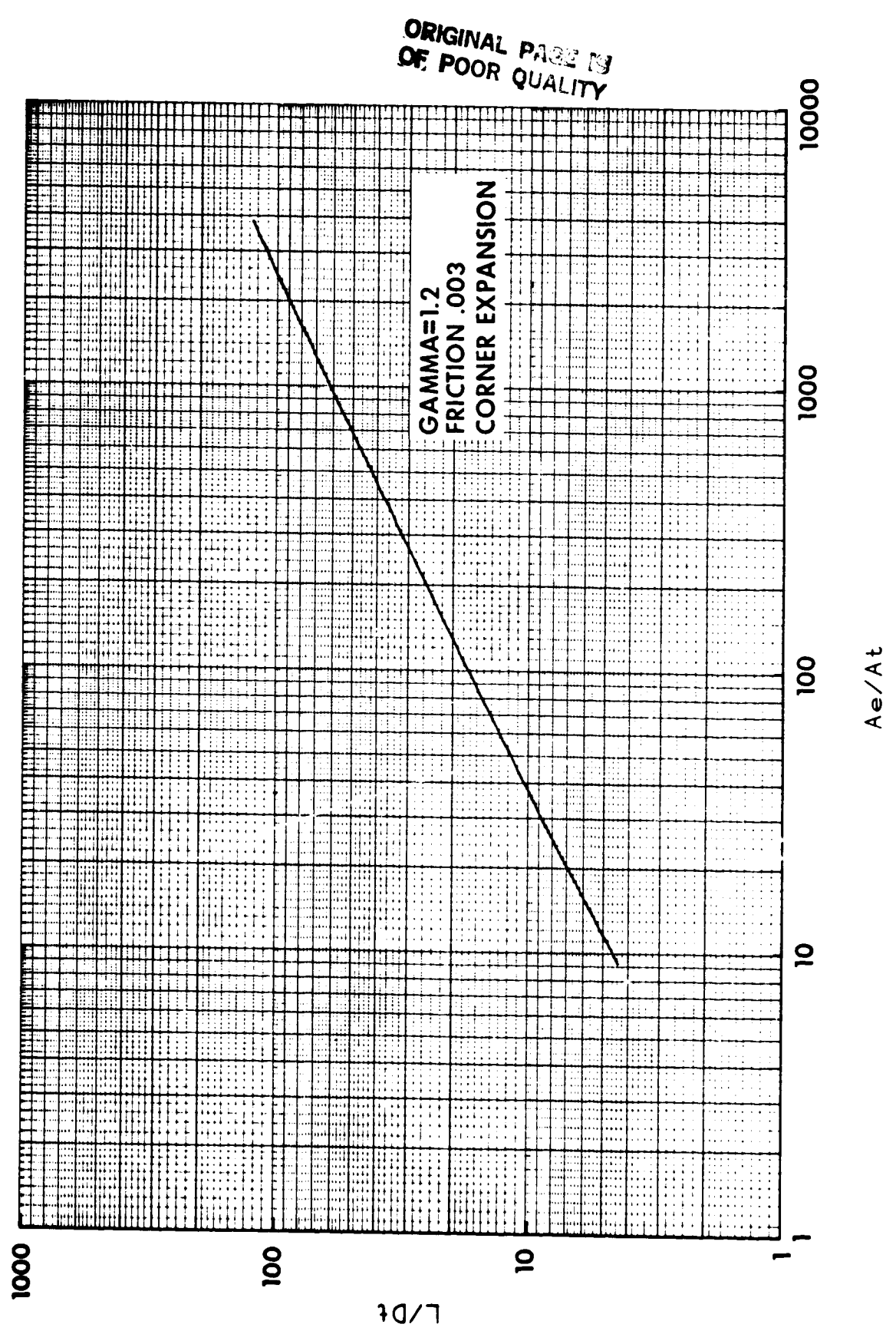


Figure 15. L/D_t versus A_e/A_t

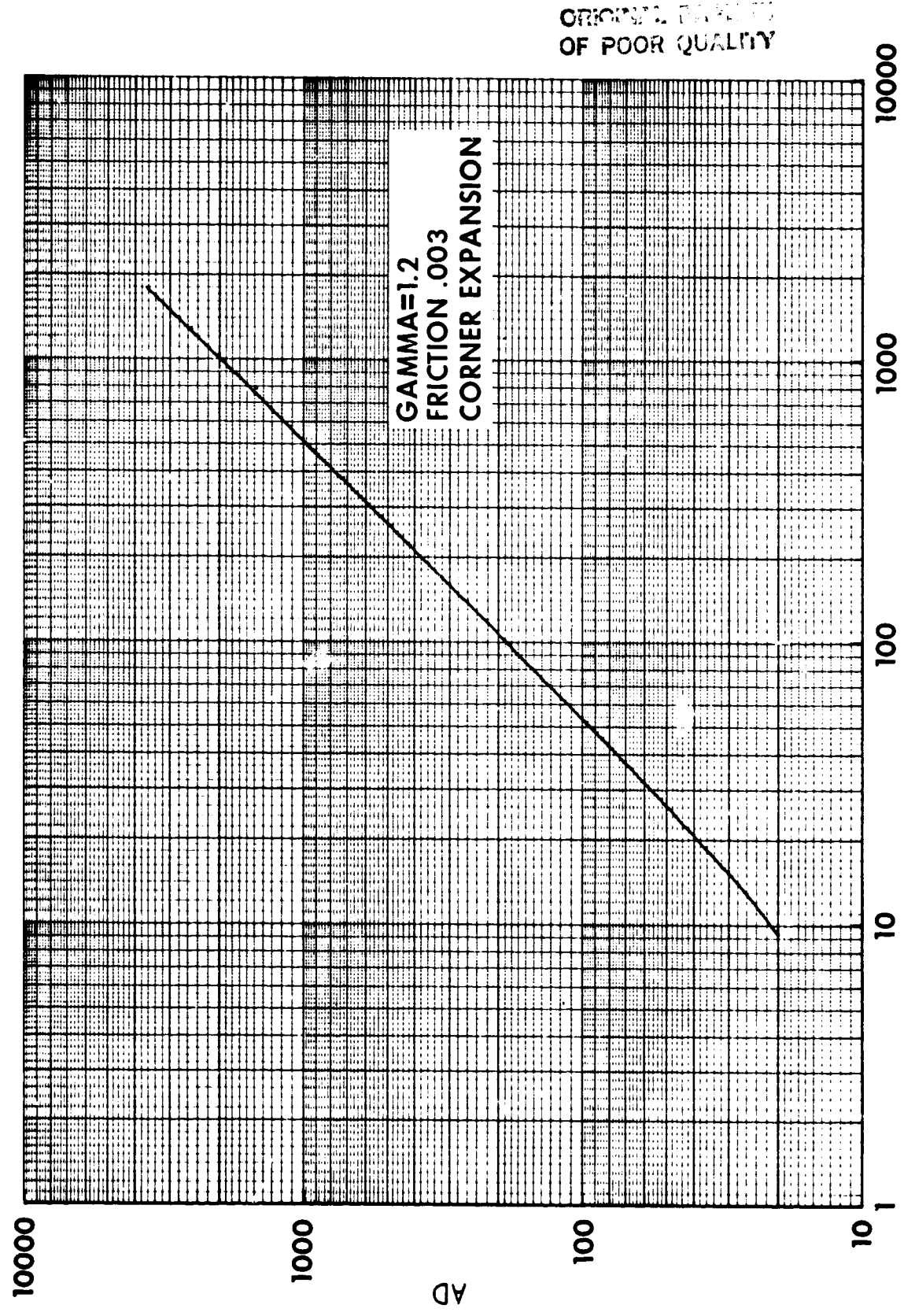


Figure 16. A_D versus A_e/A_t for minimum A_s/A_t nozzles.

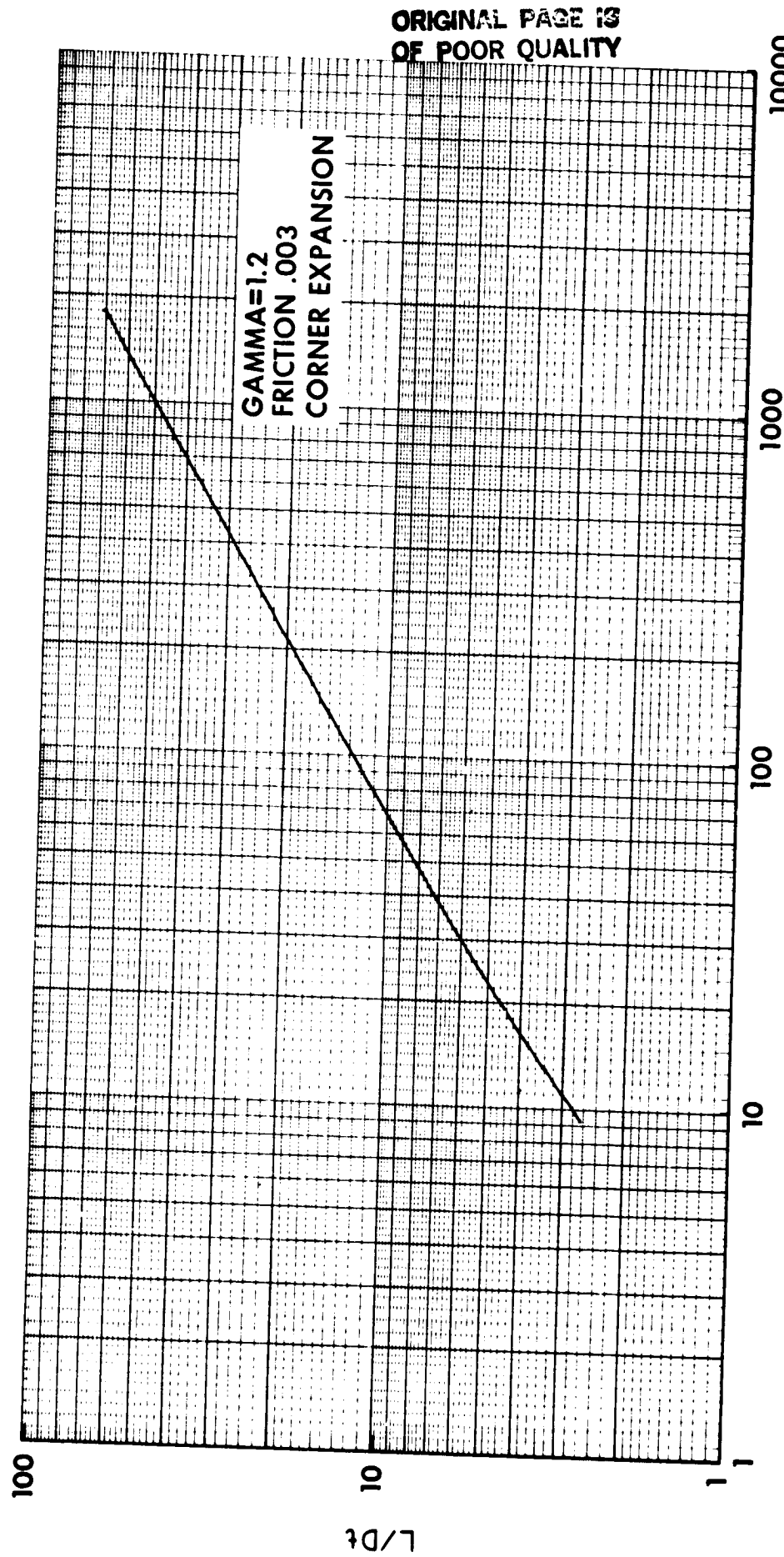


Figure 17. L/D_t versus A_e/A_t for minimum A_s/A_t nozzles.

49

ORIGINAL PAGE IS
OF POOR QUALITY

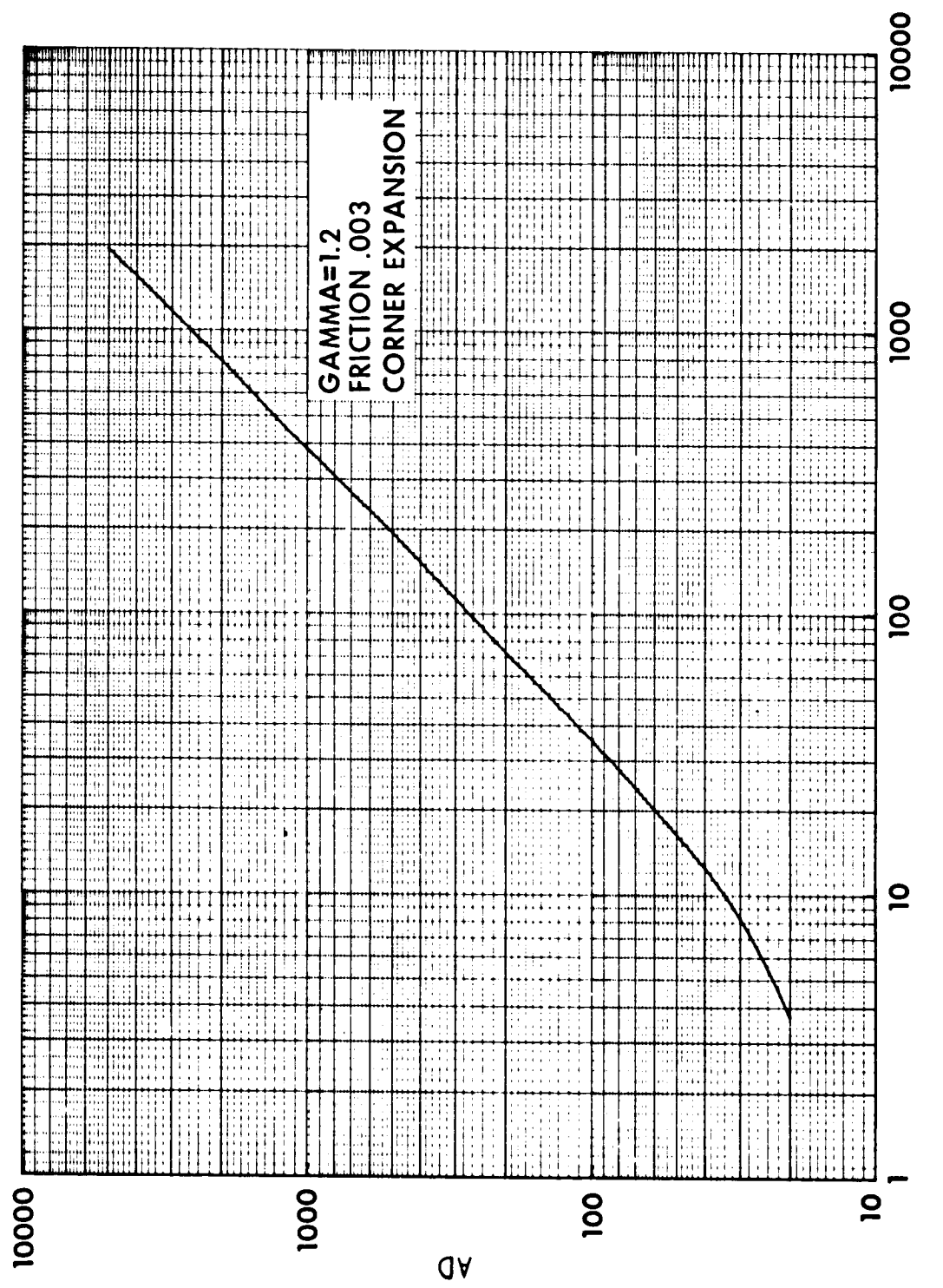


Figure 18. A_D versus A_e/A_t for minimum L/D_t nozzles.

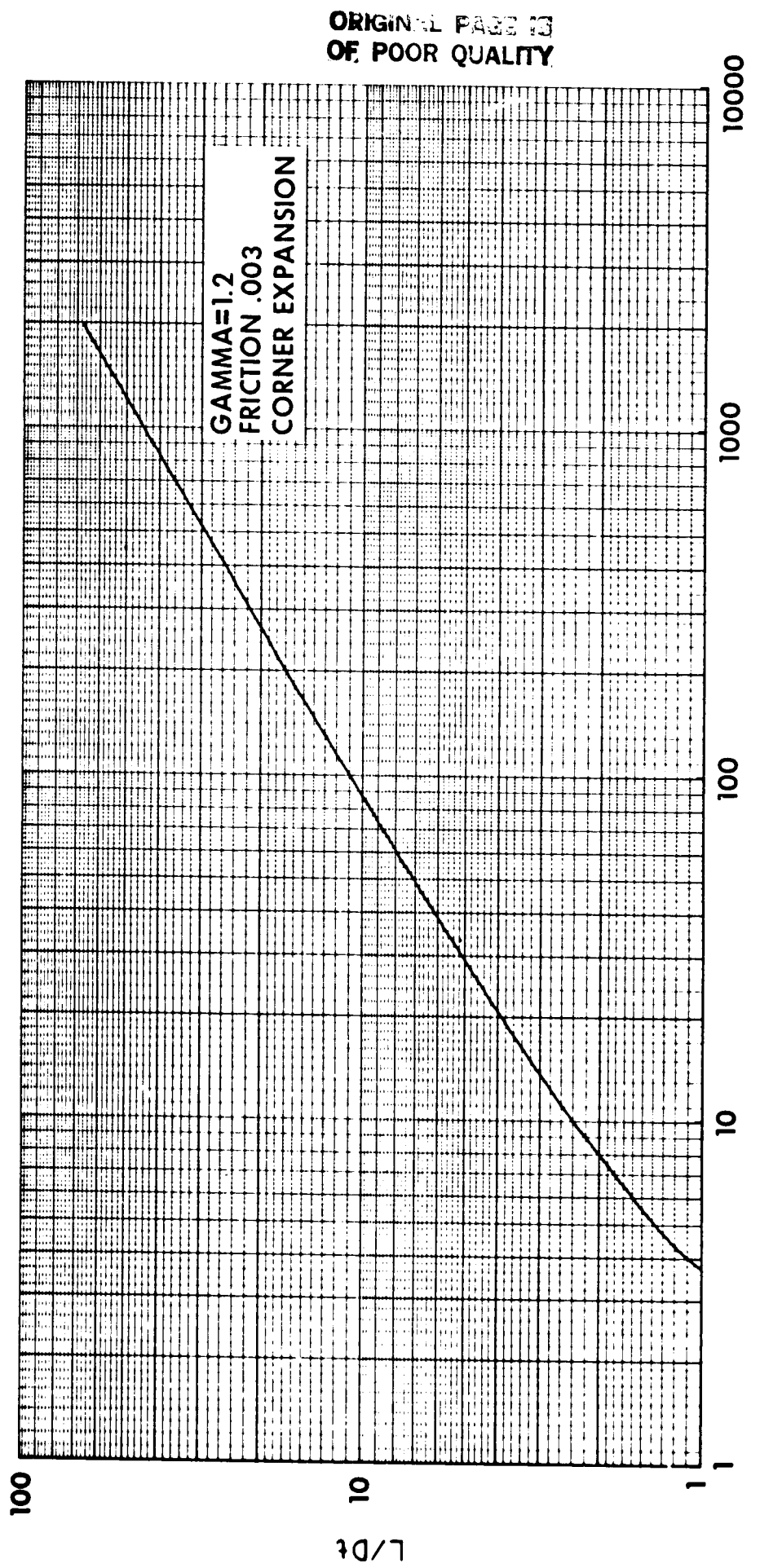


Figure 19. L/D_t versus A_e/A_t for minimum L/D_t nozzles.

REFERENCES

1. United Technologies, Pratt and Whitney Aircraft Group: Bell Nozzle Design Program. NASA Contract No. NAS9-2487, June 30, 1964.
2. Shapiro, Ascher H.: The Dynamics and Thermodynamics of Compressible Fluid Flow. New York, The Ronald Press Company, 1953.
3. Rao, G. V. R.: Exhaust Nozzle Contour for Optimum Thrust. Jet Propulsion, Vol. 28, No. 6, June 1958, pp. 377-382.